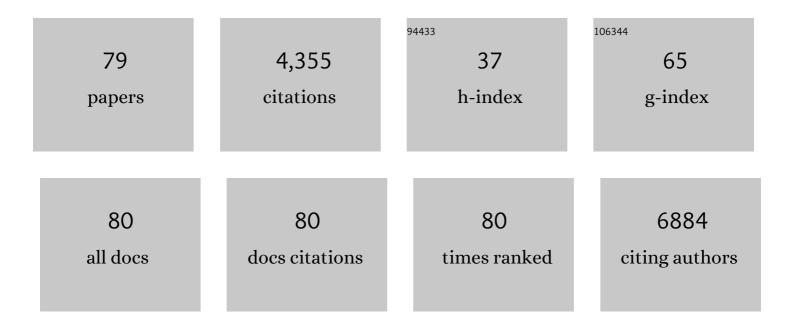
## Yuanzhi Chen

List of Publications by Year in descending order

Source: https://exaly.com/author-pdf/2274509/publications.pdf Version: 2024-02-01



YUANZHI CHEN

#	Article	IF	CITATIONS
1	Copper Nanowires as Fully Transparent Conductive Electrodes. Scientific Reports, 2013, 3, 2323.	3.3	310
2	Toward noble-metal-free visible-light-driven photocatalytic hydrogen evolution: Monodisperse sub–15 nm Ni2P nanoparticles anchored on porous g-C3N4 nanosheets to engineer 0D-2D heterojunction interfaces. Applied Catalysis B: Environmental, 2018, 221, 47-55.	20.2	251
3	Sub-5 nm Ultra-Fine FeP Nanodots as Efficient Co-Catalysts Modified Porous g-C <sub>3</sub> N <sub>4</sub> for Precious-Metal-Free Photocatalytic Hydrogen Evolution under Visible Light. ACS Applied Materials & Interfaces, 2019, 11, 5651-5660.	8.0	208
4	Preparation and magnetic properties of nickel nanoparticles via the thermal decomposition of nickel organometallic precursor in alkylamines. Nanotechnology, 2007, 18, 505703.	2.6	187
5	Ni <sub>12</sub> P <sub>5</sub> nanoparticles embedded into porous g-C <sub>3</sub> N <sub>4</sub> nanosheets as a noble-metal-free hetero-structure photocatalyst for efficient H <sub>2</sub> production under visible light. Journal of Materials Chemistry A, 2017, 5, 16171-16178.	10.3	183
6	Au–ZnO hybrid nanoflowers, nanomultipods and nanopyramids: one-pot reaction synthesis and photocatalytic properties. Nanoscale, 2014, 6, 874-881.	5.6	160
7	Construction of network-like and flower-like 2H-MoSe2 nanostructures coupled with porous g-C3N4 for noble-metal-free photocatalytic H2 evolution under visible light. Applied Catalysis B: Environmental, 2018, 233, 26-34.	20.2	147
8	Hierarchical ZnIn <sub>2</sub> S <sub>4</sub> /MoSe <sub>2</sub> Nanoarchitectures for Efficient Nobleâ€Metalâ€Free Photocatalytic Hydrogen Evolution under Visible Light. ChemSusChem, 2017, 10, 4624-4631.	6.8	140
9	Enhanced Microwave Absorption Properties by Tuning Cation Deficiency of Perovskite Oxides of Two-Dimensional LaFeO <sub>3</sub> /C Composite in X-Band. ACS Applied Materials & Interfaces, 2017, 9, 7601-7610.	8.0	123
10	Ultrafine ash aerosols from coal combustion: Characterization and health effects. Proceedings of the Combustion Institute, 2007, 31, 1929-1937.	3.9	115
11	Template-Free Synthesis of Amorphous Double-Shelled Zinc–Cobalt Citrate Hollow Microspheres and Their Transformation to Crystalline ZnCo <sub>2</sub> O <sub>4</sub> Microspheres. ACS Applied Materials & Interfaces, 2013, 5, 5508-5517.	8.0	114
12	Synthesis of Co2P/graphene nanocomposites and their enhanced properties as anode materials for lithium ion batteries. Journal of Power Sources, 2015, 295, 329-335.	7.8	111
13	Transmission Electron Microscopy Investigation of Ultrafine Coal Fly Ash Particles. Environmental Science & Technology, 2005, 39, 1144-1151.	10.0	108
14	Facile synthesis of Cu and Cu@Cu–Ni nanocubes and nanowires in hydrophobic solution in the presence of nickel and chloride ions. Nanoscale, 2013, 5, 2394.	5.6	108
15	Electron Microscopy Investigation of Carbonaceous Particulate Matter Generated by Combustion of Fossil Fuels. Energy & amp; Fuels, 2005, 19, 1644-1651.	5.1	101
16	Facile synthesis of near-monodisperse Ag@Ni core–shell nanoparticles and their application for catalytic generation of hydrogen. Nanotechnology, 2011, 22, 195604.	2.6	98
17	First application of core-shell Ag@Ni magnetic nanocatalyst for transfer hydrogenation reactions of aromatic nitro and carbonyl compounds. RSC Advances, 2013, 3, 1050-1054.	3.6	84
18	Shape-Selective Formation of Monodisperse Copper Nanospheres and Nanocubes via Disproportionation Reaction Route and Their Optical Properties. Journal of Physical Chemistry C, 2014, 118, 9801-9808.	3.1	84

Yuanzhi Chen

#	Article	IF	CITATIONS
19	Microanalysis of ambient particles from Lexington, KY, by electron microscopy. Atmospheric Environment, 2006, 40, 651-663.	4.1	82
20	Investigation of the Microcharacteristics of PM2.5in Residual Oil Fly Ash by Analytical Transmission Electron Microscopy. Environmental Science & Technology, 2004, 38, 6553-6560.	10.0	80
21	Investigation of primary fine particulate matter from coal combustion by computer-controlled scanning electron microscopy. Fuel Processing Technology, 2004, 85, 743-761.	7.2	76
22	Influence of substrate temperature on mechanical, optical and electrical properties of ZnO:Al films. Journal of Alloys and Compounds, 2010, 508, 370-374.	5.5	72
23	Structure, optical and magnetic properties of Ni@Au and Au@Ni nanoparticles synthesized via non-aqueous approaches. Journal of Materials Chemistry, 2012, 22, 2757-2765.	6.7	70
24	Co <sub>2</sub> P Nanorods as an Efficient Cocatalyst Decorated Porous gâ€C <sub>3</sub> N <sub>4</sub> Nanosheets for Photocatalytic Hydrogen Production under Visible Light Irradiation. Particle and Particle Systems Characterization, 2018, 35, 1700251.	2.3	69
25	CoO nanocrystals as a highly active catalyst for the generation of hydrogen from hydrolysis of sodium borohydride. Journal of Power Sources, 2012, 220, 391-398.	7.8	67
26	One-pot synthesis of hexagonal and triangular nickel–copper alloy nanoplates and their magnetic and catalytic properties. Journal of Materials Chemistry, 2012, 22, 8336.	6.7	66
27	Synthesis of iron–nickel nanoparticles via a nonaqueous organometallic route. Materials Chemistry and Physics, 2009, 113, 412-416.	4.0	65
28	Magnetic metal phosphide nanorods as effective hydrogen-evolution electrocatalysts. International Journal of Hydrogen Energy, 2014, 39, 18919-18928.	7.1	62
29	Preparation of hexagonal close-packed nickel nanoparticles via a thermal decomposition approach using nickel acetate tetrahydrate as a precursor. Journal of Alloys and Compounds, 2009, 476, 864-868.	5.5	60
30	Measurement of fine particulate matter using electron microscopy techniques. Fuel Processing Technology, 2004, 85, 763-779.	7.2	59
31	Emissions of Chromium, Copper, Arsenic, and PCDDs/Fs from Open Burning of CCA-Treated Wood. Environmental Science & Technology, 2005, 39, 8865-8876.	10.0	59
32	Solution-phase synthesis of nickel phosphide single-crystalline nanowires. Journal of Crystal Growth, 2009, 311, 1229-1233.	1.5	59
33	Engineering oxygen vacancies in hierarchically Li-rich layered oxide porous microspheres for high-rate lithium ion battery cathode. Science China Materials, 2019, 62, 1374-1384.	6.3	58
34	Seedâ€Induced Growth of Flowerâ€Like Au–Ni–ZnO Metal–Semiconductor Hybrid Nanocrystals for Photocatalytic Applications. Small, 2015, 11, 1460-1469.	10.0	55
35	Facile preparation and microwave absorption properties of porous Co/CoO microrods. Journal of Alloys and Compounds, 2017, 721, 411-418.	5.5	52
36	Colloidal synthesis of MoSe 2 nanonetworks and nanoflowers with efficient electrocatalytic hydrogen-evolution activity. Electrochimica Acta, 2017, 231, 69-76.	5.2	49

Yuanzhi Chen

#	Article	lF	CITATIONS
37	Lithium-rich layered oxide nanowires bearing porous structures and spinel domains as cathode materials for lithium-ion batteries. Journal of Power Sources, 2019, 418, 122-129.	7.8	40
38	Shape-dependent magnetic and microwave absorption properties of iron oxide nanocrystals. Materials Chemistry and Physics, 2017, 192, 339-348.	4.0	35
39	Shape-related optical and catalytic properties of wurtzite-type CoO nanoplates and nanorods. Nanotechnology, 2014, 25, 035707.	2.6	32
40	Controllable synthesis of Cu–Ni core–shell nanoparticles and nanowires with tunable magnetic properties. Chemical Communications, 2016, 52, 6918-6921.	4.1	30
41	Effect of Component Distribution and Nanoporosity in CuPt Nanotubes on Electrocatalysis of the Oxygen Reduction Reaction. ChemSusChem, 2015, 8, 486-494.	6.8	28
42	Electron transport properties of magnetic granular films. Science China: Physics, Mechanics and Astronomy, 2013, 56, 15-28.	5.1	25
43	From a Au-rich core/PtNi-rich shell to a Ni-rich core/PtAu-rich shell: an effective thermochemical pathway to nanoengineering catalysts for fuel cells. Journal of Materials Chemistry A, 2018, 6, 5143-5155.	10.3	25
44	Size- and Structure-Controlled Synthesis and Characterization of Nickel Nanoparticles. Journal of Nanoscience and Nanotechnology, 2009, 9, 5157-5163.	0.9	22
45	Solution synthesis of triangular and hexagonal nickel nanosheets with the aid of tungsten hexacarbonyl. CrystEngComm, 2016, 18, 1295-1301.	2.6	22
46	Characterization of Ambient Airborne Particles by Energy-Filtered Transmission Electron Microscopy. Aerosol Science and Technology, 2005, 39, 509-518.	3.1	19
47	Preparation of monodisperse Ni nanoparticles and their assembly into 3D nanoparticle superlattices. Materials Chemistry and Physics, 2014, 147, 604-610.	4.0	19
48	Cu@Ni core–shell nanoparticles prepared via an injection approach with enhanced oxidation resistance for the fabrication of conductive films. Nanotechnology, 2020, 31, 355601.	2.6	19
49	MoSe2-Ni3Se4 Hybrid Nanoelectrocatalysts and Their Enhanced Electrocatalytic Activity for Hydrogen Evolution Reaction. Nanoscale Research Letters, 2020, 15, 132.	5.7	19
50	Synthesis of Ni–Au–ZnO ternary magnetic hybrid nanocrystals with enhanced photocatalytic activity. Nanoscale, 2015, 7, 11371-11378.	5.6	17
51	Phase-controlled synthesis and magnetic properties of cubic and hexagonal CoO nanocrystals. Nanotechnology, 2016, 27, 455602.	2.6	17
52	Preparation of multi-branched Au–ZnO hybrid nanocrystals on graphene for enhanced photocatalytic performance. Materials Letters, 2015, 161, 379-383.	2.6	15
53	Colloidal synthesis of Cu–ZnO and Cu@CuNi–ZnO hybrid nanocrystals with controlled morphologies and multifunctional properties. Nanoscale, 2016, 8, 11602-11610.	5.6	15
54	Preparation of porous Li1.2Mn0.54Ni0.13Co0.13O2 micro-cubes for high-capacity lithium-ion batteries. Journal of Alloys and Compounds, 2020, 834, 155152.	5.5	15

YUANZHI CHEN

#	Article	IF	CITATIONS
55	A facile approach to fabrication of well-dispersed NiO–ZnO composite hollow microspheres. RSC Advances, 2013, 3, 24430-24439.	3.6	14
56	A Nonaqueous Approach to the Preparation of Iron Phosphide Nanowires. Nanoscale Research Letters, 2010, 5, 786-790.	5.7	11
57	Injection synthesis of Ni–Cu@Au–Cu nanowires with tunable magnetic and plasmonic properties. Chemical Communications, 2013, 49, 11545.	4.1	11
58	Monodisperse core-shell Li4Ti5O12@C submicron particles as high-rate anode materials for lithium-ion batteries. Electrochimica Acta, 2021, 390, 138874.	5.2	11
59	Blue-luminescent hafnia nanoclusters synthesized by plasma gas-phase method. Materials Chemistry and Physics, 2011, 130, 823-826.	4.0	10
60	Synthesis and photocatalytic properties of multi-morphological AuCu3-ZnO hybrid nanocrystals. Nanotechnology, 2015, 26, 415602.	2.6	8
61	Chemical Synthesis of Monodisperse Fe–Ni Nanoparticles via a Diffusion-Based Approach. Journal of Nanoscience and Nanotechnology, 2010, 10, 3053-3059.	0.9	7
62	Transition from paramagnetism to ferromagnetism in HfO2 nanorods. Journal of Applied Physics, 2013, 113, 076102.	2.5	7
63	A facile solution approach for the preparation of Ag@Ni core–shell nanocubes. Materials Letters, 2014, 116, 239-242.	2.6	7
64	Investigation on the self-assembly of gold nanoparticles into bidisperse nanoparticle superlattices. Colloids and Surfaces A: Physicochemical and Engineering Aspects, 2015, 480, 11-18.	4.7	7
65	Electrical transport properties in Co nanocluster-assembled granular film. Journal of Applied Physics, 2017, 121, .	2.5	6
66	Nickel Colloidal Superparticles: Microemulsion-Based Self-Assembly Preparation and Their Transition from Room-Temperature Superparamagnetism to Ferromagnetism. Journal of Physical Chemistry C, 2021, 125, 5880-5889.	3.1	6
67	High-frequency magnetic characteristics of Fe-Co-based nanocrystalline alloy films. Science China Technological Sciences, 2010, 53, 1501-1506.	4.0	5
68	Preparation of Bimetallic Core-shell Nanoparticles with Magnetically Recyclable and High Catalytic Abilities. Procedia Engineering, 2012, 36, 504-509.	1.2	5
69	Hot-injection synthesis of Ni-ZnO hybrid nanocrystals with tunable magnetic properties and enhanced photocatalytic activity. Journal of Nanoparticle Research, 2017, 19, 1.	1.9	5
70	Tungsten hexacarbonyl-induced growth of nickel nanorods and nanocubes. Materials Letters, 2018, 229, 340-343.	2.6	5
71	Preparation of Anisotropic Transition Metal Phosphide Nanocrystals: The Case of Nickel Phosphide Nanoplatelets, Nanorods, and Nanowires. Journal of Nanoscience and Nanotechnology, 2010, 10, 5175-5182.	0.9	4
72	High Frequency Characteristics of Fe65Co35 Alloy Cluster-Assembled Films Prepared by Energetic Cluster Deposition. Journal of Nanoscience and Nanotechnology, 2011, 11, 11119-11123.	0.9	4

YUANZHI CHEN

#	Article	IF	CITATIONS
73	Solution preparation of alloy core–shell nanoparticles: The case of Ni–Cu@Au–Cu nanoparticles. Materials Letters, 2013, 99, 180-183.	2.6	4
74	Photocatalysis: Co2 P Nanorods as an Efficient Cocatalyst Decorated Porous g-C3 N4 Nanosheets for Photocatalytic Hydrogen Production under Visible Light Irradiation (Part. Part. Syst. Charact. 1/2018). Particle and Particle Systems Characterization, 2018, 35, 1870003.	2.3	4
75	Preparation of LiNi0.5Mn1.5O4 cathode materials by using different-sized Mn3O4 nanocrystals as precursors. Journal of Solid State Electrochemistry, 2022, 26, 1359-1368.	2.5	3
76	Gas-phase synthesis and magnetism of HfO2 nanoclusters. European Physical Journal D, 2013, 67, 1.	1.3	2
77	Magnetic Properties of Oxygen-doping Fe-Co-based Nanocrystalline Alloy Films for High Frequency Application. Procedia Engineering, 2012, 36, 516-520.	1.2	1
78	Influence of surface and interface modification on the electrical transport behaviors in Co@Cu nanocomposite films. Journal of Magnetism and Magnetic Materials, 2018, 460, 34-40.	2.3	1
79	High frequency characteristics of Fe <inf>65</inf> Co <inf>35</inf> alloy cluster-assembled films prepared by energetic cluster deposition. , 2010, , .		Ο